On the usage of electron beam as a tool to produce radioactive isotopes in photo-nuclear reactions.

G. G. Bunatian [a], V. G. Nikolenko and A. B. Popov

Joint Institute for Nuclear Research, 141980, Dubna, Russia

(Dated: December 23, 2010)

Abstract

We treat the bremsstrahlung induced by initial electron beam in converter, and the production of a desirable radio-isotope due to the photo-nuclear reaction caused by this bremsstrahlung. By way of illustration, the yield of a number of some, the most in practice applicable, radio-isotopes is evaluated. The acquired findings persuade us that usage of modern electron accelerators offers a practicable way to produce the radio-isotopes needful nowadays for various valuable applications in the nuclear medicine.

PACS numbers: PACS number(s): 25.20.-x

Keywords: radio-isotope production, nuclear medicine.

[a] Email: bunat@cv.jinr.dubna.ru

1. Introduction

Nowadays, it is rather impossible to find any branch of science, industry, medicine, forensic, asf, in which the radio-isotopes are not widely used [1–6]. Although there is a series of unstable natural isotopes arising from the decay of primordial uranium and thorium, the most of about 200 radio-isotopes used for now on a regular basis are produced artificially. Despite all the nuclear reactors produce the manifold radio-isotopes as a result of fission of ^{235}U contained in their fuels, the recovery of these radio-isotopes is extremely problematic issue, and they would not be received for primary applications, especially for medical use. At present radio-isotope marketable production is primarily brought about by exposition of the appropriate element to neutrons in a nuclear reactor, or to charged particles, like protons, deuterons, or alpha particles, in a cyclotron [7]. As a general rule, it is far more difficult to make a radio-isotope in a cyclotron than in a reactor. Cyclotron nuclear reactions are less productive and less predictable than ones performed in a reactor. The variety of cyclotron-produced radio-isotopes is tightly restricted too. Economic factors would also militate against cyclotron production. In fact, it proves to be anyway not competitive with the reactor radio-isotope production.

As to reactor-based manufacturing, there are two processes to produce isotopes: fission of ^{235}U by neutrons within an exposed target, with subsequent recovery of a desirable isotope out of fission fragments, and neutron capture by nucleus of an appropriate sample, which results in elaboration of a required isotope [7]. The ^{235}U fission cross-section σ_{nf} is well known to be at least a factor of about 100 greater than the typical neutron capture $A(Z,N)(n,\gamma)A'(Z,N+1)$ cross-section to produce some radio-isotope $A'(Z,N+1)$ that could other-ways be recovered from ^{235}U fission fragments. That is why the radio-isotope consumers community world-through dismissed the neutron capture as a viable process for production of the primary needful radio-isotopes in quantities required to meet global demand, thought this process could be used to make minor radio-isotope amounts to provide a stable domestic supply. For instance, in Russia different radio-isotopes, including ^{99}Mo/^{99m}Tc, are produced on the Leningrad power station using the neutron capture reactions in the channel of the $RBMK$-1000 reactor [8].

Thus, in these days, the most of world's production of primary radio-isotopes is carried

provide a thermal neutron flux $(10^{14} - 10^{15})$n/(sec cm^2), and are fueled with low enriched uranium (LEU), or in some cases with (HEU) as well [7]. These reactors have become indispensable for the industrial production of marketable radio-isotopes, in particular medical isotopes to supply the rapidly increasing demand for diagnostic and therapeutic procedures based on nuclear medicine techniques. The nuclear-medicine community defines the medical isotopes to include first of all the isotope ^{99}Mo, that is the precursor to the short-living ^{99m}Tc that's used in $\approx 85\%$ of all the nuclear medicine procedures worldwide, and also ^{131}I,^{133} X and other manifold radioactive materials used to produced radiopharmaceuticals [2, 4, 7, 9, 10]. The medical radio-isotope recovery is humanly the most vital outcome of nuclear physics and industry.

The supply reliability of radio-pharmacies, hospitals, clinics and outpatients centers with the radio-isotopes is currently the primary concern of world nuclear-medicine community [7]. In actual fact, recent experience suggests that unplanned emergent reactor shutdowns would cause severe supply disruption. A number of contingence incidents during last years has been pointing up unreliability in the supply of medical radio-isotopes, particular ^{99}Mo/^{99m}Tc. Some 95% of the world's supply of these comes from only five reactors, all of them are over 40 years old [7]. So the greatest single threat to supply reliability is the approaching obsolescence of the aging reactors that current large-scale producers utilize to irradiate HEU targets to elaborate the needful radio-isotopes. Last years, there took place a number of significant disruptions in medical radio-isotope supply, some of which have been lasting by now [7, 11]. For instance, the concern about the long-term supply of medical radio-isotopes has been exacerbated when the shutdown of research reactor HFR in the Netherlands since August 2008 has caused ^{99}Mo shortage world-wide. The most productive and oldest, yet a while ago refurbished, Canada's NRU reactor was shutdown in the summer 2009 [12], after the heavy water leak was discovered in May 15, 2009. It is not clear if and when the NRU could be restarted, or how to make up for its outage. The worldwide supply of radio-isotopes is likely to be unreliable unless newer production sources come on line.

Besides posing a threat to patients treatment, the current method used by the world's main producers increases the menace of nuclear terrorism, as it employs weapons-grade HEU. So the burning question is now to eliminate, or at least minimize, the HEU use in reactor fuel, irradiated targets, and production facilities. Only very few small-scale producers, *e.g.*

the LEU targets [7]. The bulk of consumed radio-isotopes are still obtained utilizing HEU and, to the best of knowledge, the conversion to the LEU targets is not believed before long. Especially the radio-isotope producing community had been counting on the to-be-built reactors $MAPLE1$ and $MAPLE2$, and on the related processing facilities at Chalk-River site, Canada, which would not have used the HEU. Yet the $MAPLE$s, designed as a replacement for NRU, did not perform as contemplated, and in May 2008 Atomic Energy of Canada Ltd. made the decision to end the $MAPLE$'s project [13]. This has, in fact, put on hold any plans to convert to LEU-based large-scale radio-isotope production. Instead, the world community these days needs both new radio-isotope production inventions and the facilities that will continue work safely in the long term, without using weapon-grade uranium.

In this respect, we treat in what follows the photo-production of various radio-isotopes, Sections 3, 4, which is due to the bremsstrahlung induced in converter by initial electron beam of electron accelerator, Section 2. Also we consider, in Section 5, the case when a desirable isotope results in decaying a parent radio-isotope that stems itself in the photo-production. At last, in Section 6, the all-round discussion of findings persuades us that the most preferable way to produce radio-isotopes is the usage of electron beams provided by modern electron accelerators. What encourages our work is the exploration by now carried out in the Fefs. [14–17].

2. Bremsstrahlung in converter

As was proclaimed above, the purpose is to acquire how to work out the various radio-isotopes, needful to-day for manifold applications in technology, science and medicine, by making use of electron beams delivered by microtrons, linear electron accelerators, etc. That beam, with an electron energy distribution $\rho_e(E_e)$ and a current density $J_e(t)[\mathrm{A/cm^2}]$ (generally speaking, time dependent), travels through the converter (see Fig. 1), which is prepared of some proper heavy element, such as W, Pt etc.The bremsstrahlung is thereby induced with current density

$$J_\gamma(E_\gamma) = \frac{\mathcal{N}_\gamma(E_\gamma)}{} \tag{2.1}$$

expressed in terms of the photon number $\mathcal{N}_\gamma(E_\gamma)$ with the energy $E_\gamma = |\mathbf{k}| = k$, per $1\mathrm{cm}^2, 1\mathrm{s}, 1\,\mathrm{MeV}$.

In turn, that γ-ray flux, interacting with respective nuclei of the sample (see Fig. 1), induces the photo-nuclear reaction

$$\gamma + A(Z,N) \Longrightarrow A'(Z,N-1) + n, \tag{2.2}$$

so that a desirable isotope $A'(Z,N-1)$ comes out. Certainly, this process (2.2) can only be realized, if the energy E_γ of γ rays is, at least, greater than the neutron binding energy B_n of a considered nucleus $A(Z,N)$, $E_\gamma > B_n \approx 8\,\mathrm{MeV}$. Actually, the isotope $A(Z,N-1)$ production process will successfully run provided E_γ is of the order of, and comes over the energy E_{GR} of giant resonance in the photo-nuclear reactions (2.2) on respective nuclei, $E_\gamma \gtrsim E_{GR}(Z,N) \sim 13 \div 19$ MeV [18]. As a matter of course, an electron must have got the energy $E_e > E_\gamma$ in order to give rise to the bremsstrahlung with the required energy E_γ. Thus, only the processes involving the electron and photon energies

$$\mathrm{E}_\gamma\,,\; E_e \gtrsim E_{GR} \tag{2.3}$$

are to be taken into consideration and explored, which is the key point of our treatment. Next, we limit the current study by the condition

$$E_e \leq 100\,\mathrm{MeV} \tag{2.4}$$

as well. The guide relations (2.3), (2.4) govern all the presented calculations, specifying the energy area where the acquired findings hold true. Also, in the ordinary way, all the evaluations we make in the work are the first $\alpha-$order, and we abandon contributions from all the high α-order processes.

In passing across converter, a high energy electron is primarily known to lose its energy (see e.c. Refs. [19–21]) due to the bremsstrahlung by scattering in the fields of nuclei of heavy atoms of converter. As the relation (2.3) holds, the angular distribution of scattered electrons as well as emitted photons has got a sharp maximum in momentum direction of an initial electron. Both electrons and photons spread within a small, rather negligible solid angle $\Theta \sim m/E_e$ around direction of the initial electron momentum [19–21]. Then, with proper

between the momenta of incident electron and emitted photon, a very handy expression for the cross-section to describe the photon energy distribution results (see *e.g.* Refs. [20, 22, 23]):

$$\frac{\mathrm{d}\sigma_b(k)}{\mathrm{d}k} = \frac{2Z_C^2}{137} r_0^2 \frac{1}{k} \times$$
$$\times\{\left(\frac{E_e^2 + {E'_e}^2}{E_e^2} - \frac{2E'_e}{3E_e}\right) \cdot \left(\ln M + 1 - \frac{2}{b}\arctan b\right) + \tag{2.5}$$
$$+\frac{E'_e}{E_e}\left(\frac{2}{b^2}\ln(1+b^2) + \frac{4(2-b^2)}{3b^3}\arctan b - \frac{8}{3b^2} + \frac{2}{9}\right)\} \,,$$

where $k = E_\gamma$ stands for the energy of radiated γ-quantum, $E'_e = E_e - k$, Z_C is the atomic number of the converter material, and

$$b = \frac{2E_e E'_E Z^{1/3}}{C\,m\,k} \,, \quad \frac{1}{M} = \left(\frac{m\,k}{2E_e E'_e}\right)^2 + \frac{Z_C^{2/3}}{C^2} \,, \quad C = 111 \,, \quad r_0 = \frac{e^2}{m} = 2.818 \cdot 10^{-13}\,\mathrm{cm}.$$

Besides the aforesaid bremsstrahlung in the field of nucleus, there exists the bremsstrahlung by scattering an incident electron by atomic electrons. For a fast electron, $E_e \gg m$, the cross section of this process is known to coincide with the bremsstrahlung cross section on nucleus with $Z = 1$ [19–21]. Then, the atomic electrons contribution into the whole electron bremsstrahlung is taken into account just by replacing the factor Z_C^2 in Eq. (2.5) by $Z_C(Z_C + \delta)$ with $\delta \lesssim 1$. As for heavy converter atoms $Z_C \gg 1$, this correction is rather of very small value.

The bremsstrahlung, with all the feasible energies $k = E_\gamma$, causes the mean energy loss of electron on a unit of path [19, 20]

$$-\frac{\mathrm{d}E_e(x)}{\mathrm{d}x} = \mathcal{N}_C \cdot E_e(x) \cdot \varphi_{rad}(E_e), \tag{2.6}$$

The number $\mathcal{N}_C$ of scattering atoms of converter in $1\,\mathrm{cm}^3$ is

$$\mathcal{N}_C = \frac{\rho_C \cdot 6.022 \cdot 10^{23}}{A_C}, \tag{2.7}$$

where ρ_C is the density of converter material, and A_C is its atomic weight. The quantity φ_{rad} is written in the form

The coefficient K_C, very slightly varying with the energy E_e, provided $E_e \gtrsim 10$ MeV, can be found in Refs. [19, 20, 24] for various heavy atoms. So, upon passing a path x, an electron with initial energy $E_e(0)$ will have got, in consequence of the radiative losses, the energy

$$E_{e\,rad}(x) \approx E_e(0) \exp[-x\mathcal{N}_C\varphi_{rad}]. \tag{2.9}$$

In fast electrons, $E_e \gg m$, elastic scattering on heavy nuclei of converter, the angular distribution has got a very sharp maximum, within the solid angle $\Theta < (m/E_e)^2$, and therefore can be leaved out of our consideration [19–21].

In treating the fast electron collision with atomic electrons, without photon emitting, we are to consider two cases. Firstly, let the momentum Δ_I transferred to an atomic electron be

$$\Delta_I \lesssim I_Z \approx 13.5 Z_C \mathrm{eV}, \tag{2.10}$$

the ionization potential of atom. Apparently, as $\Delta_I \ll E_e$, a scattering angle is negligible. The mean electron energy loss on a unit of path, caused by its inelastic collisions with atoms, is described by the expression (see Refs. [19, 20, 23])

$$-\frac{\mathrm{d}E_e(x)}{\mathrm{d}x} = 2\pi r_0^2 m\mathcal{N}_C Z_C \ln\frac{E_e^3(x)}{2mI_Z^2}\,, \tag{2.11}$$

which can be rewritten in the form

$$x = -\frac{1}{6\pi r_0^2 m\mathcal{N}_C Z_C}\int\limits_{E_e(0)}^{E_{e\,I}(x)} \frac{\mathrm{d}E}{\ln[E(2mI_Z^2)^{-1/3}]}\,, \tag{2.12}$$

where $E_e(0)$ is the electron energy at the starting edge of converter, and $E_{e\,I}(x)$ stands for the electron energy upon passing the distance x, which is caused by the ionization losses. With the conditions (2.3), (2.4), we can actually presume

$$\ln E \approx \ln E_e^{av}\,, \quad E_e^{av} = \frac{E_e(0) + E_{GR}}{2} \tag{2.13}$$

in the Eq. (2.12). Then we arrive at the estimation of the energy loss on the distance x due to the inelastic electron collisions with atoms

Secondly, when, unlike (2.10), the momentum transferred $\Delta_I \gg I_Z$, yet still $\Delta_I \ll E_e$ anyway, atomic electrons can be considered as free ones, and the fast electron interaction with they reduces to the elastic forward scattering on free resting electrons [19, 21], which causes no energy loss, as a matter of fact.

Amenably to Eqs. (2.9), (2.12)-(2.14), the electron with the incident energy $E_e(0)$ at the starting edge of converter has got the energy

$$E_e(x) \approx E_{e\,rad}(x) - \frac{6\pi r_0^2 m Z_C \ln[E_e^{av}(2mI_Z^2)^{-1/3}]}{\varphi_{rad}}\Big(1 - \frac{E_{e\,rad}(x)}{E_e(0)}\Big) \approx$$
$$\approx E_{e\,rad}(x) + \Delta E_{e\,I}(x)\,, \qquad (2.15)$$

upon passing the path x through converter (see Fig. 1). Just this, x-dependent, energy $E_e(x)$ is to be substituted into Eq. (2.5) to describe the bremsstrahlung of an electron at the distance x from the starting edge of converter. Thus, the bremsstrahlung production cross-section (2.5) turns out to be function of the distance x, via the electron energy $E_e(x)$ (2.15).

In the actual evaluation explicated further in Sections 3, 4, the converter thickness R_C proves to be chosen so that there are no electrons with the energies $E_e(R_C) \gtrsim 10\,\mathrm{MeV} \gg m$ at the final edge of converter.

As expounded above, only the bremsstrahlung with $k \gtrsim 10$ MeV $\gg m$, described by Eq. (2.5), is of value to induce the desirable photo-nuclear reaction (2.2). This bremsstrahlung, caused by the initial electron beam with the energy distribution $\rho_e(E_e)$ and the current density $J_e(t)$, when stems at a distance x from the starting edge of converter, is described by the photon current density (2.1)

$$J_\gamma(x, k, E_e, Z_C, \rho_C, t) = \rho_e(E_e) J_e(t) \mathcal{N}_C \frac{\mathrm{d}\sigma_b(k, E_e(x), Z_C)}{\mathrm{d}k}\,, \qquad (2.16)$$

where the cross section $\mathrm{d}\sigma_b/\mathrm{d}k$ is given by Eq. (2.5) with the electron energy $E_e(x)$ (2.15). This γ-flux spreads then forward, as was explicated above.

In this bremsstrahlung passing the path $(R_C - x)$ from a point x up to the final edge of converter R_C (see Fig. 1), there are three processes which cause the continuing γ-ray absorption [19–21] : 1) the e^+e^--pairs production; 2) the photo-effect; 3) the Compton

$k \gtrsim 10$ MeV [19–21]. Consequently, the bremsstrahlung current density $J_\gamma(x,k)$ (2.16) decreases, becoming at the final edge of converter

$$J_\gamma(x,k,R_C) = J_\gamma(x,k)\cdot\exp\Big(-\frac{R_C-x}{l_C(Z_C,\mathcal{N}_C,k,\rho_C)}\Big)\,, \tag{2.17}$$

where the length of absorption l consists from three aforesaid parts

$$\frac{1}{l_C} = \frac{1}{l_{pair}} + \frac{1}{l_{photo}} + \frac{1}{l_{Com}}\,. \tag{2.18}$$

Generally speaking, a tiny small quantity $1/l_{\gamma n}$, caused by the reactions like (2.2), should have been added to right-hand side of Eq. (2.18), for conscience's sake. The values of l for various materials are found, for instance, in Refs. [20, 24]. Let us mention that we deal with the γ-ray energies just above the so-called "area of maximum transparency" [19, 20, 24].

As understood, precision of all the carried out calculations is proved to be at least of the order $\sim \frac{m}{E_{GR}}$, $\sim \frac{I_Z}{E_{GR}}$, that is anyway none the worse than $\sim 10\%$.

With taken into consideration the restrictions imposed by the guide conditions (2.3), (2.4), we shall now discuss how the cascade of electrons and photons, practicable to the isotope production (2.2), would emerge. The processes in those an electron with the energy $E_e < E_{GR}$ participates can't anyway lead to any discernible contribution into the photo-neutron production (2.2) of the desired isotope $A'(Z,N-1)$. In slowing-down from the initial energy $E_e(0)$ to the energy E_{GR}, an electron loses the energy

$$\tilde{\Delta} \approx E_e(0) - E_{GR}\,. \tag{2.19}$$

This energy loss $\tilde{\Delta}$ itself isn't considered to be small. So, at the maxima currently treated electron energy $E_e(0) = 100\,\mathrm{MeV}$, we would have got $\tilde{\Delta} \approx 85\,\mathrm{MeV}$, and for the timely most vital $E_e(0) = 50\,\mathrm{MeV}$ we would arrive at $\tilde{\Delta} \approx 35\,\mathrm{MeV}$. As generally received [20, 25], the primary share of this energy lost $\tilde{\Delta}$ is radiated most probably as the $\gamma-$rays with energies

$$\tilde{k} = \tilde{E}\gamma \approx \frac{\tilde{\Delta}}{2}\,. \tag{2.20}$$

Only a small part of this energy loss $\tilde{\Delta}$ is emitted as a flux of comparatively soft photons, and $\gamma-$radiating with the energies $k = E_\gamma > \tilde{k}$ proves to be all the more negligible [20, 25]. As was already discussed above, in absorbing a photon with the considerable energy $\tilde{k}$ (2.20),

$$E^+ \approx E^- \approx \frac{\tilde{k}}{2} \approx \frac{\tilde{\Delta}}{4}\,. \tag{2.21}$$

Surely, there is no reason to suggest these energies to be as small as negligible, yet anyway they are nevertheless substantially smaller than the initial electron energy $E_e(0)$. Thus for the timely most vital case $E_e(0) = 50\,\mathrm{MeV}$, we have got $E^\pm \approx 8\,\mathrm{MeV} < E_{GR}$, so that the thereby produced e^+, e^- can never contribute to the isotope production (2.2) at all, which is understood in observing Fig. 2. Put another way, there would be a cascade, but the particles participating therein would have got energies beyond the key condition (2.3). At the largest initial electron energy we currently consider (2.4), $E_e(0) = 100\,\mathrm{MeV}$, there would be $E^\pm \approx 20\,\mathrm{MeV}$, so as, generally speaking, these e^+, e^- themselves would give rise to the bremsstrahlung which could in turn serve to the isotope $A'(Z, N-1)$ photo-neutron production (2.2). Yet this isotope production, caused by those secondary electrons with energies $E^\pm \approx 20\,\mathrm{MeV}$, is anyway 10 times as small as the production due to the initial electrons with $E_e(0) = 100\,\mathrm{MeV}$ themselves, which comes to light in observing the findings presented in tables 5,6,7, Section 4. Thus, when we abandon, even at $E_e(0) = 100\,\mathrm{MeV}$, the above explicated cascade, the thereby inherent ambiguouties will never come over $\approx 10\%$. That is why we do not draw into consideration the bremsstrahlung which would be induced, in converter or in sample, by the electrons those themselves would be originated by absorption of the bremsstrahlung, which in its turn is due to scattering an initial electron on nuclei in converter.

Upon integrating Eq. (2.17) over the initial electron energy distribution and over the converter length, we obtain the bremsstrahlung flux at the final edge of converter

$$J_{\gamma\,C}(k, R_C, Z_C, \rho_C, E_E^b, E_e^u, \Delta_e, t) = \int\limits_{E_e^b}^{E_e^u} \mathrm{d}E \int\limits_0^{R_C} \mathrm{d}x J_\gamma(x, k, R_C, E, Z_C, \rho_C, t)\,, \tag{2.22}$$

where E_e^b, E_e^u are, respectively, the bottom and upper energies of the electron distribution in beam, and Δ_e is to describe its width. In our further actual evaluations, the electron energy varies between the limits E_e^b, E_e^u, and we choose

$$\varphi_e(E) = \frac{1}{\Delta_e}\exp[-((E-\bar{E})/\Delta_e)^2], \quad \bar{E} = \frac{E_e^b + E_e^u}{2} \tag{2.23}$$

$$1 = \int\limits_{E_e^b}^{E_e^u} \mathrm{d}E \rho_e(E)\,.$$

Surely, when $\Delta_e \to 0$, Eq. (2.23) reduces to the δ-function electron energy distribution. Also, let us recall the initial electron current density J_e in Eqs. (2.16), (2.17), (2.22) is given in $\mathrm{A/cm^2} = 10^{19}\mathrm{e^-}/(1.602 \cdot \mathrm{sec} \cdot \mathrm{cm^2})$ where $\mathrm{e^-}$ is the electron electric charge.

3. Radio-isotope photo-production in sample

Traveling forward, the bremsstrahlung flux (2.22) intrudes into the sample (see Fig. 1) that incorporates the isotope $A(Z,N)$ which serves to produce the desirable radio-isotope $A'(Z,N-1)$ due to the photo-nuclear reaction (2.2). As well known, this process is caused by the giant resonance in the nuclear photo-absorption [18]. By now, there exist numerous reliable measurements of the cross-sections $\sigma_{\gamma\,n}(k,Z,N)$ of the neutron γ-production (2.2) for manifold nuclei. The respective data are put to use in our evaluations. The errors in these $\sigma_{\gamma n}$ measurements may rather amount $\sim 10\%$, which puts a bound to the accuracy attainable in our evaluations. If anything, it is to point out that at the large converted $\gamma-$ray energies, $E_\gamma \gtrsim 30\,\mathrm{MeV}$, the contribution to (2.2) from area beyond the giant-resonans nuclear photo-absorption would be discernible because at these energies there exists the nuclear photo-absorption due to the surface absorption, the virtual quasi-deuteron absorption, and the absorption caused by the nucleon polarizability in nucleus [26]. Though this contribution ought to have been taken into account, its impact onto the quantities we have been considering were hardly more than a few per cent, even at $E_e(0) = 100\,\mathrm{MeV}$.

Absorption of the γ-flux goes on inside sample in much the same way as in converter, yet l_C (2.18) gives place to $l_S(Z_S, \mathcal{N}_S, \rho_S, k)$ of the sample. Upon passing a distance y from the starting edge of sample (see Fig. 1), the γ-flux (2.22) modifies as follows

$$J_{\gamma\,S}(y,k,R_C,Z_C,\rho_C,E_e^b,E_e^u,\Delta_e,t) =$$
$$= J_{\gamma\,C}(k,R_C,Z_C,\rho_C,E_E^b,E_e^u,\Delta_e,t)\exp[-\frac{y}{l_S(Z_S,\mathcal{N}_S,\rho_S,k)}]\,. \qquad (3.1)$$

Then the density of atoms $\mathcal{N}_{ris}(y,k,Z,N-1,t)$ of the desirable radio-isotope $A'(Z,N-1)$, produced per 1s by the current density (3.1), with a given k, at the distance y (see Fig.1) is

$$\frac{\mathrm{d}\mathcal{N}_{ris}(y,k,Z,N-1,t)}{\mathrm{d}t} =$$
$$= \mathcal{N}_S(Z,N)\cdot\sigma_{\gamma\,n}(k,Z,N)\cdot J_{\gamma\,S}(y,k,R_C,Z_C,\rho_C,E_e^b,E_e^u,\Delta_e,t)\,, \tag{3.2}$$

where the density of sample atoms

$$\mathcal{N}_S(Z,N) = \frac{\rho_S\cdot 6.022{\cdot}10^{23}}{A_S} \tag{3.3}$$

is given in terms of the sample density ρ_S and the atomic weight A_S. When the isotope $A(Z,N)$, needful to produce $A'(Z,N-1)$, constitutes only some part $\mathcal{A}_{bn}$ of the sample material, the density ρ_S in (3.3) is

$$\rho_S(Z,N) = \mathcal{A}_{bn}\bar{\rho}_S\,, \tag{3.4}$$

where $\bar{\rho}_S$ is the whole sample density, in particular the density of the natural element A_S. Unlike, the quantity l_S in Eq. (3.1) is determined by the total density $\bar{\rho}_S$ anyway.

Upon integrating the quantity (3.2) over the length of sample and over the photon energy k, we come to describe the total amount of radio-isotope produced inside the sample, per 1 s, per 1cm^2 of a sample area,

$$\frac{\mathrm{d}\mathcal{N}_{ris}(Z,N-1,t)}{\mathrm{d}t} = J_e(t)\cdot\mathcal{N}^0_{ris}(Z,N-1)\,, \tag{3.5}$$

$$\mathcal{N}^0_{ris}(Z,N-1) = \mathcal{N}_S(Z,N)\cdot\mathcal{N}_C(Z_C,N_C)\times$$
$$\times\int\limits_{E_e^b}^{E_e^u}\mathrm{d}E\rho_e(E)\int\limits_0^{R_C}\mathrm{d}x\int\limits_0^{\infty}\mathrm{d}k\Big(\frac{\mathrm{d}\sigma_b(k,E_e(x),Z_C)}{\mathrm{d}k}\Big)\sigma_{\gamma\,n}(k,Z,N)\times$$
$$\times\left(1-\exp\Big(-\frac{R_S}{l_S(k,Z_S,N_S)}\Big)\right)\cdot l_S(k,Z_S,N_S)\times$$
$$\times\exp\Big(-\frac{R_C-x}{l_C(k,Z_C,N_C)}\Big)\,. \tag{3.6}$$

The integration over the photon energy k is actually restricted by the area where the product

$$\Big(\frac{\mathrm{d}\sigma_b(k)}{\mathrm{d}k}\Big)\cdot\sigma_{\gamma\,n}(k) \tag{3.7}$$

has got a discernible value. Beyond any questions, the values $k\lesssim B_n$ and $k\gtrsim E_e$ contribute

The expression (3.5) represents a source to produce this isotope $A'(Z, N-1)$. To proceed further, we are to recall that the produced radio-isotope $A'(Z, N-1)$ is not stable, and its decay is governed by the life-time τ_s, so that a number of decays per 1s reads ordinarily

$$\frac{\mathcal{N}_{ris}(t, \tau_s)}{\tau_s}.$$

Yet the isotope $A'(Z, N-1)$ itself undergoes irradiation by the same $\gamma-$flux (3.1) as the original isotope $A(Z, N)$ does. Then the photo-nuclear reaction

$$\gamma + A'(Z, N-1) \to A''(Z, N-2) + n \tag{3.8}$$

results in depletion of the elaborated desired isotope $A'(Z, N-1)$,

$$-\mathcal{N}_{ris}(t, \tau_s) \frac{J_e(t)\, \mathcal{N}^0_{ris}(Z, N-1)}{\mathcal{N}_S(Z, N)}\,. \tag{3.9}$$

Then, amenably to the common equation

$$\frac{\mathrm{d}\mathcal{N}_{ris}(t, \tau_s)}{\mathrm{d}t} = J_e(t)\mathcal{N}^0_{ris}(Z, N-1) - \frac{\mathcal{N}_{ris}(t, \tau_s)}{\tau_s} - \\ -\mathcal{N}_{ris}(t, \tau_s) \frac{J_e(t)\, \mathcal{N}^0_{ris}(Z, N-1)}{\mathcal{N}_S(Z, N)}\,, \tag{3.10}$$

we obtain the radio-isotope amount, per $1\mathrm{cm}^2$ area of the sample, elaborated during an exposition time T_e

$$\mathcal{N}_{ris}(T_e, \tau_s) = \mathcal{N}^0_{ris} \int\limits_0^{T_e} \mathrm{d}t J_e(t) \exp[t/\tilde{\tau}_s] \cdot \exp[-T_e/\tilde{\tau}_s]\,, \tag{3.11}$$

$$\frac{1}{\tilde{\tau}_s(J_e(t))} = \frac{1}{\tau_s} + \frac{J_e(t)\, \mathcal{N}^0_{ris}(Z, N-1)}{\mathcal{N}_S(Z, N)}\,. \tag{3.12}$$

Although, strictly speaking, the cross-section $\sigma_{\gamma n}(k, Z, N)$ in the expression $\mathcal{N}^0_{ris}$ in Eq. (3.9), and in the last terms in Eqs. (3.10), (3.12) would give place to $\sigma_{\gamma n}(k, Z, N-1)$, we utilize here $\sigma_{\gamma n}(k, Z, N-1) \approx \sigma_{\gamma n}(k, Z, N)$ in the evaluations of these correction terms. For a time-independent initial electron current J_e, Eq. (3.11) reduces to

When $T_e \ll \tau_s$, this gets simplify, giving just

$$\mathcal{N}_{ris}(T_e, \tau_s) = \mathcal{N}^0_{ris} J_e T_e \,. \tag{3.14}$$

Let us mention that though the correction (3.9) is to be allowed for, its impact on the isotope production is very small, rather negligible, at the values of T_e, J_e currently treated.

It is to designate that we have been using, all over the carried out calculations, just the life-time τ, yet not the so-called half-decay period $T_{1/2} = \tau \ln 2$.

It is generally accepted (see, for instance, Refs. [14–17, 27]) to describe the radio-isotope production in terms of the yield $Y[\mathrm{Bq}/(\mathrm{h} \cdot \mu\mathrm{A} \cdot \mathrm{mg} A(Z,N))]$ of the produced activity in Bq per 1h of exposition time, per 1μA of the initial electron current, and per 1mg of the isotope $A(Z,N)$ in the sample, which serves to produce the desirable isotope $A'(Z, N-1)$. Accordingly its definition, this characteristic Y is expressed through the quantity (3.11)

$$Y = \frac{\mathcal{N}_{ris}(Z, N-1, J_e, E^b_e, E^u_e, R_C, R_S, \mathcal{A}_{bn}, T_e, \tau_s)}{R_S(\mathrm{cm}) \cdot \rho_S(\mathrm{mg/cm^3}) A(Z,N) \cdot \tau_s(\mathrm{s}) \cdot T_e(\mathrm{h}) \cdot J_e(\mu\mathrm{A})} \,. \tag{3.15}$$

It is also of use to discuss the total yield of activity produced by the initial electron current J_e inside the whole actual sample, with 1cm^2 area and thickness R_S, during exposition time T_e

$$\mathcal{Y}(\mathrm{Bq}) = Y \cdot R_S(\mathrm{cm}) \cdot \bar{\rho}_S(\mathrm{mg/cm^3}) \cdot \mathcal{A}_{bn} \cdot J_e(\mu\mathrm{A}) \cdot T_e(\mathrm{h}) \,. \tag{3.16}$$

Beside Y, $\mathcal{Y}$ (3.15), (3.16), it is of value to consider the total amount of radio-isotope $A'(Z, N-1)$ elaborated in the whole sample

$$\mathcal{M}_{Z,N-1}(\mathrm{g}) = \frac{\mathcal{N}_{ris}(Z, N-1, J_e, E^b_e, E^u_e, R_C, R_S, \mathcal{A}_{bn}, T_e, \tau_s) \cdot \mathcal{A}_{bn} \cdot (Z+N-1)}{6.022{\cdot}10^{23}} \,, \tag{3.17}$$

where $(Z + N - 1) = A - 1$ is the corresponding atomic weight. In Sections 4 and 5, we display the results of Y and $\mathcal{M}$ evaluations. Apparently, a $\mathcal{Y}$ value is directly expressed through a Y value accordingly (3.16).

$$A(Z,N)+\gamma = A'(Z,N-2)+2n\,, \tag{3.18}$$

$$A(Z,N)+\gamma = A'(Z-1,N)+p\,, \tag{3.19}$$

$$A(Z,N)+\gamma = A'(Z-1,N-1)+p+n \tag{3.20}$$

are generally known to take place as well. Yet their thresholds are nearly twice as much as the threshold of the reaction (2.2), and their cross-sections are about ten times as small as the cross-section of the reaction (2.2) [18]. So, with accuracy quite sufficient, the processes (3.18), (3.19), (3.20) are not competitive with the considered main photo-production (2.2) of the isotope $A'(Z,N-1)$. Surely, when desired, the yield of isotopes $A'(Z,N-2)$, $A'(Z-1,N-1)$, $A'(Z-1,n)$ from irradiated sample would be calculated as well.

Let us recall that the eventual results (3.11)-(3.17) are governed by the manifold parameters, which characterize 1) the initial electron beam, $J_e, T_e, \bar{E}_e, E_e^b, E_e^u, \Delta_e$; 2) the converter, $\sigma_b, \mathcal{N}_C, \rho_C, R_C, l_C, K_C$; 3) the sample and the produced radio-isotope, $\sigma_{\gamma\,n}, \mathcal{N}_S, \rho_S$, $Z_S, N_S, \mathcal{A}_{bn}, l_S, R_S, N, Z, \tau_s$. In involving these quantities into consideration, the proper discussions were explicated above. The dependence of $Y, \mathcal{M}, \mathcal{Y}$ on these parameters will be considered in next Section 4 for some radio-isotopes, produced immediately in the reaction (2.2). Thereafter, in Section 5, we inquire into the event that the decay

$$A'(Z,N-1) \Longrightarrow A^m(Z',N') \tag{3.21}$$

of this, at the first step obtained radio-isotope $A'(Z,N-1)$, serves, in turn, as a source to produce the second-step radio-isotope A^m, which is eventually put to use in manufacturing the needful practicable preparation.

4. Evaluation of the radio-isotope production characteristics

Now we evaluate the quantities $Y, \mathcal{M}, \mathcal{Y}$, acquired above, for some examples, which typify the radio-istope production using the electron beam. All over further consideration, the converter is presumed to be prepared of ^{nat}W (the natural tungsten) with a varying thickness R_W(cm), and three cases will be considered: the production of ^{99}Mo , ^{237}U , ^{117m}Sn, with varying the sample thickness $R_{\rm Mo}$, $R_{\rm U}$, $R_{\rm Sn}$, the initial electron energy E_e and the current

electron current provided by the electron linear accelerator or microtron. The purpose is to visualize the dependence of the production characteristics $Y, \mathcal{M}, \mathcal{Y}$ (3.15)-(3.17) on the aforesaid parameters.

First of all we treat the reaction

$$\gamma + {}^{100}\mathrm{Mo} \Longrightarrow {}^{99}\mathrm{Mo} + n \tag{4.1}$$

providing the production of the isotope ^{99}Mo, which is known to be the most applicable [4, 7], as discussed in Introduction. Let us recall the ^{99}Mo life-time $\tau_{^{99}\mathrm{Mo}} \approx 96$h.

As indicated by Eqs. (3.18), (3.19), (3.20), the isotopes ^{98}Mo, ^{98}Nb, ^{99}Nb could be recovered as well, if required.

In order to elucidate the key point of treatment, we display in Fig. 2. the γ-flux $J_{\gamma C}(k)$ (2.22) at the various thickness R_{W} of W-converter and at the various initial electron energy (2.23). The behavior of $J_{\gamma C}(k)$ is to be correlated with the energy dependence of the cross-section of the reaction (4.1) [28]. As understood, only the area of k-values where $J_{\gamma C}$ and $\sigma_{\gamma n}$ overlap determines the evaluated quantities (3.5)-(3.17) to describe the radio-isotope ^{99}Mo production, which we are treating now. The γ-rays with energies k beyond this area are out of value. As the function $\sigma_{\gamma n}$ is well known to be, more or less, of the same form and magnitude for all the heavy and middle weight nuclei, Fig. 2 typifies the calculation of radio-isotope production by means of electron beam.

As explicated in Section 2, the simultaneous treatment of botch bremsstrahlung production and absorption and electron energy losses serves to realize how the isotope yield does depend on the converter thickness R_{W}. This dependence is typified by table 1. As understood there exists the most preferable R_{W}-value for given material of the converter and the incident electron energy. In actual radio-isotope manufacturing, just this R_C is to be utilized. Let us mention that the quantity $Y \approx 3.2\,\mathrm{kBq}/(\mathrm{h}\,\mu\mathrm{A}\ \mathrm{mg}^{100}\mathrm{Mo})$ was obtained in Ref. [14] at $R_{\mathrm{W}} = 0.3$cm, which is some greater than the most preferable value $R_{\mathrm{W}} \approx 0.17$cm. As seen, the result of Y measurement in Ref. [14] does actually coincide with ours in table 1, with a reasonable accuracy.

The dependence of $Y, \mathcal{M}$ on the R_S value at the various electron energies E_e gets understood from the data given in the tables 2, 3, 4. This Y , $\mathcal{M}$ behaviour is due to simultaneous run of the isotope ^{99}Mo photo-production and the γ-rays absorption in the Mo sample, as

stantially slower than linearly. That is why the quantity Y decreases, and $\mathcal{M}$ tends to some limit by increasing $R_{\rm Mo}$.

The quantity $\mathcal{Y}$ (3.16) behaves rather alike $\mathcal{M}$. With the same parameters, as in table 3, for the natural ^{nat}Mo sample, $\rho_{\rm Mo} = 9,8{\rm g/cm}^3, \mathcal{A}_{bn} = 0.1$, with the thickness $R_{\rm Mo} = 2{\rm cm}$ and $1{\rm cm}^2$ area, during 1h exposition time, we have got

$$\mathcal{Y}_{^{99}{\rm Mo}} \approx 1.7 \cdot 10^{10}{\rm kBq}\,, \tag{4.2}$$

which is rather noteworthy. If anything, by dividing the yield (3.16) on total sample mass, one might treat the so-called specific activity $\mathcal{Y}^{sp}_{^{99}{\rm Mo}}$, which measures the activity of ^{99}Mo per unit mass of reaction products,

$$\mathcal{Y}^{sp}_{^{99}{\rm Mo}} = \frac{\mathcal{Y}_{^{99}{\rm Mo}}}{\rho_{^{99}{\rm Mo}} \cdot R_{^{99}{\rm Mo}} \cdot 1{\rm cm}^2} \approx 10^9 \frac{\rm kBq}{\rm g}. \tag{4.3}$$

Yet this quantity would be rather of small use, as it does actually depend on the sample and converter parameters, $R_C, R_S, Z_C, Z_S, \rho_C, \rho_S$, the exposition time T_e, the percetage $\mathcal{A}_{bn}$ of ^{100}Mo in the sample, and so on. That is why we have been making use of $\mathcal{Y}_{^{99}{\rm Mo}}$ itself without having recourse to $\mathcal{Y}^{sp}_{^{99}{\rm Mo}}$ (4.3).

Fig. 3 offers the time dependence of the quantities Y (3.15) and $\mathcal{M}$ (3.17). They represent the produced activity and mass as a function of exposition time T_e in hours. With T_e increasing, the quantity $\mathcal{N}_{ris}$ grows tangibly slower than linearly. Consequently, $Y(T_e)$ decreases and $\mathcal{M}(T_e)$ tends to a finite limit when T_e increases. As seen, there is no reason for too long exposition time.

Table 5 demonstrates how the quantities $R_{\rm W}$, Y and $\mathcal{M}$ depend on the initial electron energy. As seen, the most preferable $R_{\rm W}$ value increases smoothly with electron energy growth. The feature to emphasize is the sharp augmentation of Y, $\mathcal{M}$ in coming from $\bar{E}_e = 20$ MeV to $\bar{E}_e = 25$ MeV and then to $\bar{E}_e = 50$ MeV, yet the relatively slower enhancement shows up by increasing $\bar{E}_e$ from $\bar{E}_e = 50$ MeV to $\bar{E}_e = 100$ MeV.

The next example of considerable practical interest [29] is the photo-production of the tin isomer radio-isotope ^{117m}Sn

$$\gamma + {}^{118}{\rm Sn} \Longrightarrow {}^{117m}{\rm Sn} + n\,. \tag{4.4}$$

We put to use the cross-section of this reaction acquired from Ref. [30]. The results of Y

for various thicknesses $R_{\rm W}$ and $R_{\rm Sn}$ of the W converter and of the natural tin ^{nat}Sn sample, with 1cm^2 area. Let us recall that the isotope ^{118}Sn constitutes about 24% of the natural tin, that is $\mathcal{A}_{bn} \approx 0.24$ in (3.4), $\bar{\rho}_{\rm Sn} = 7{\rm g/cm}^3$, and the isomer ^{117m}Sn life time $\tau_{^{117m}{\rm Sn}} \approx 20.2$d [24]. As seen, this table 6 offers the same dependence of Y (3.15) and $\mathcal{M}$ (3.17) on the electron energy for the ^{117m}Sn production, as the table 5 for the production of ^{99}Mo does. Accordingly to the data in this table 6, the quantity $\mathcal{Y}$ (3.16) at $\bar{E}_e = 50$ MeV, $R_{\rm Sn} = 2$cm proves to be

$$\mathcal{Y}_{^{117m}{\rm Sn}} \approx 0.8 \cdot 10^{10}{\rm kBq}\,, \tag{4.5}$$

which is of the same order, as the $\mathcal{Y}$ (4.2) for ^{99}Mo production.

At last, we discuss the production of the widely applied [31], specifically in the nuclear fuel research, radio-isotope ^{237}U,

$$\gamma + {}^{238}{\rm U} \Longrightarrow {}^{237}{\rm U} + n\,. \tag{4.6}$$

The cross section of this reaction is acquired from Ref. [32]. All the consideration runs in much the same way as in the cases of treating the ^{99}Mo and ^{117m}Sn production. Yet now we evaluate the quantities Y (3.15), $\mathcal{M}$ (3.17) not just at the time T_e, the finish of the exposition, but in one day after the 5h-long irradiation. The reason to do so is that the experimental measurements of the ^{237}U production were carried out in Ref. [15] just under such conditions. Apparently, as the time of observation T, counting from the start of irradiation, is longer than the exposition time T_e, the quantities (3.15), (3.17) are to be replaced by

$$Y(T) = Y(T_e)\exp[-(T - T_e)/\tau_{^{237}{\rm U}}]\,, \tag{4.7}$$

$$\mathcal{M}(T) = \mathcal{M}(T_e)\exp[-(T - T_e)/\tau_{^{237}{\rm U}}]\,, \tag{4.8}$$

with the ^{237}U life time $\tau_{^{237}{\rm U}} = 6.75$d, $T - T_e = 1$d, which are presented in table 7. For the parameters utilized in Ref. [15], $R_{\rm W} = 0.3$cm, $\bar{E}_e = 24$ MeV, $\Delta_e \to 0$, we have got $Y_{\rm U} \approx 1.35\,{\rm kBq/(h\,\mu A\,mg^{238}U)}$, which is in accordance with the result obtained in [15], $Y_{\rm U} \approx 1.1\,{\rm kBq/(h\,\mu A\,mg^{238}U)}$. Let us recall the isotope ^{238}U constitutes 99.276% of the natural U, that is $\mathcal{A}_{bn} \approx 1$ in (3.4), (3.16), (3.17), and $\rho_{\rm U} = 18.7{\rm g/cm}^3$. Then, utilizing the data from table 7, and choosing $\bar{E}_e = 50$ MeV, $R_{\rm U} = 2$cm, $T_e = 5$h (unlike the cases of

$$\mathcal{Y}_{^{237}\mathrm{U}} \approx 35 \cdot 10^{10}\mathrm{kBq}\,, \tag{4.9}$$

that is still more significant than the $\mathcal{Y}$ values for ^{99}Mo and ^{117}Sn, (4.2), (4.5).

5. Production of a practicable radio-isotope via an isotope-precursor

In a number of important cases, a radio-isotope of practical use $A^m(Z', N')$ is generated by decaying

$$A'(Z, N-1) \Longrightarrow A^m(Z', N') + e^{\pm} \tag{5.1}$$

an isotope $A'(Z, N-1)$ obtained in the photo-nuclear reaction (2.2), which was described in previous Section 4. Thus, the parent isotope decay (5.1) is now a source to produce a needful eventual radio-isotope $A^m(Z', N')$ with a life-time τ_m. The density of atoms $\mathcal{N}^m_{ris}$ of this isotope A^m produced by the γ-flux (3.1) inside a given sample is then described by the common equation

$$\frac{\mathrm{d}\mathcal{N}^m_{ris}(t, \tau_s, \tau_m)}{\mathrm{d}t} = p_m \frac{\mathcal{N}_{ris}(t, \tau_s)}{\tau_s} - \frac{\mathcal{N}^m_{ris}(t, \tau_s, \tau_m)}{\tau_m}\,. \tag{5.2}$$

Here p_m stands to allow for the fact that the isotope decay (5.1) constitutes a share p_m of all the possible decays of $A(Z, N-1)$. Amenably Eq. (5.2) we generally obtain the amount of radio-isotope $A^m(Z', N')$ for the sample with 1cm^2 area, at the total time T, counting from the exposition start,

$$\mathcal{N}^m_{ris}(T, \tau_s, \tau_m) = p_m \frac{\exp[-T/\tau_m]}{\tau_s} \int\limits_0^T \mathrm{d}t \exp[t/\tau_m] \mathcal{N}_{ris}(t, \tau_s)\,, \tag{5.3}$$

with the quantity $\mathcal{N}_{ris}(t, \tau_s)$ given by Eqs. (3.10)-(3.14). Ordinarily, we are dealing with the practicable case $T \geq T_e$. In calculating $\mathcal{N}^m_{ris}$ (5.3), we have abandoned leaking the isotope $A^m(Z', N')$ due to the feasible photo-nuclear reaction $A^m(Z', N')(\gamma, n)A''(Z', N'-1)$ during exposition time T_e. In the case a constant initial electron current J_e irradiates converter during the exposition time T_e, and afterwards disappears, the general Eq. (5.3) reduces to

$$\mathcal{N}^m_{ris}(T, T_e, \tau_s, \tau_m) = \mathcal{N}^0_{ris} J_e p_m \frac{\tilde{\tau}_s}{\Big(} \exp[-T/\tau_m] \Big(\tau_m \Big(\exp[T_e/\tau_m] - 1 \Big) -$$

$$-\tau_-\Big(\exp[T_e/\tau_-]-1\Big)+\tau_-\Big(1-\exp[-T_e/\tilde{\tau}_s]\Big)\Big(\exp[T/\tau_-]-\exp[T_e/\tau_-]\Big)\Big)\Big)\,, \qquad (5.4)$$

$$\frac{1}{\tau_-}=\frac{1}{\tau_m}-\frac{1}{\tilde{\tau}_s}\,.$$

With replacing the quantity $\mathcal{N}_{ris}(T_e,\tau_s)$ in Eqs. (3.15)-(3.17) by $\mathcal{N}^m_{ris}(T,T_e,\tau_s,\tau_m)$ (5.3), (5.4), and τ_s by τ_m as well, the quantities Y^m and $\mathcal{M}^m$ are defined to describe the eventual isotope $A^m(Z',N')$ production.

Hereafter, using the Eq. (5.4), we treat the production of the most extensively employed radio-isotope ^{99m}Tc [4, 7], which stems in the ^{99}Mo $\beta-$decay

$$^{99}\mathrm{Mo}\longrightarrow{}^{99m}\mathrm{Tc}+e^-\,. \qquad (5.5)$$

The branching of the $\beta-$decay of ^{99}Mo into the isomer ^{99m}Tc, with the life-time $\tau_m\approx$10h , amounts $\approx 85\%$, that is $p_m\approx 0.85$ in Eq. (5.4) [33]. In other cases ^{99}Mo decays giving the practically stable ^{99}Tc isotope with $\tau_{\mathrm{Tc}}\approx 4\cdot 10^5$y [14, 24, 33]. All the results presented hereafter are obtained for the Mo sample of 1cm^2 area, as had been doing in previous Sections 2, 3, 4.

Tables 8, 9 show that for a given T_e there exists the most preferable time T_{max}, counting from the exposition start, when the yield of ^{99m}Tc activity Y_{Tc^m} and the mass $\mathcal{M}_{\mathrm{Tc}^m}$ have got their maxima. Therefore the radio-isotope ^{99m}Tc is to be extracted out of the Mo sample upon the time T_{max} best of all. This fact is thought to be of a practical value, though the dependence of Y_{Tc^m} and $\mathcal{M}_{\mathrm{Tc}^m}$ yield on T sees to be rather smooth.

Table 10 shows the activity yield Y_{Tc^m} decreases and the mass $\mathcal{M}_{\mathrm{Tc}^m}$ tends to a certain limit as the thickness R_{Mo} of Mo sample increases. That is so because the quantity $\mathcal{N}^m_{ris}$ (5.3) increases substantially slower than linearly, just alike the quantity $\mathcal{N}_{ris}$ (3.11) does.

Tables 11, 12 figure the quantities $Y_{\mathrm{Tc}^m}(T)$, $\mathcal{M}_{\mathrm{Tc}^m}(T)$ calculated at $T=T_e$ and $T=T_{max}$, for the various initial electron energies $\bar{E}_e$ (attached by the associated parameters E^b_e , E^u_e , Δ_e as in table 5), with choosing the most preferable values of the converter thickness R_{W} and the time T_{max} for each $\bar{E}_e$. It is of interest to correlate the results obtained for the Mo foil, $R_{\mathrm{Mo}}=0.01$cm, with those for the thick enough Mo sample, $R_{\mathrm{Mo}}=2$cm. Just for that matter, the evaluation firstly carried out at $R_{\mathrm{Mo}}=0.01$cm is then replicated at $R_{\mathrm{Mo}}=2$cm, with the results offered in tables 11 and 12, respectively.

Accordingly the data in table 12, the radio-isotope production characteristic $\mathcal{Y}$ (3.16),

$$\mathcal{Y}_{\mathrm{Tc}^m}(T_{max}) \approx 1.2 \cdot 10^{10}\mathrm{kBq}\,, \tag{5.6}$$

that is of the same order as the corresponding value (4.2) for ^{99}Mo. In other words, let one irradiate the natural ^{nat}Mo sample, with the 1cm^2 area and the thickness $R_{\mathrm{Mo}} = 2$cm, during $T_e = 1$h by the γ-flux originated by the electron beam, with $\bar{E}_e = 50\,\mathrm{MeV}$ and $J_e = 1\mathrm{A/cm}^2$, in the ^{nat}W converter with the thickness $R_{\mathrm{W}} = 0.3$cm. Then, the ^{99}Mo activity (4.2) would be elaborated by the end of exposition, and, in turn, the ^{99m}Tc activity (5.6), comparable with (4.2), would be generated at the time $T_{max} = 23.5$h

It is to mention that upon extracting the isotope ^{99m}Tc out of the Mo sample at $T = T_{max}$, the next amount of ^{99m}Tc isotope, comparable with that at $T = T_{max}$, would be accumulated in the Mo sample in $T_1 \approx \tau_{^{99m}\mathrm{Tc}} \ln(\tau_{^{99}\mathrm{Mo}}/\tau_{^{99m}\mathrm{Tc}}) \approx 23$h, as can be realized from Eq. (5.4). Yet further repeatedly, over and over again, withdrawing ^{99m}Tc out of the sample is usually thought to be rather of less efficiency because of diminishing the ^{99}Mo amount.

Of course, the examples treated in the presented work do not cover all the area of the radio-isotope application in these days. In particular, there exists a number of practicable isotopes eligible to be wrought up by the method described hereupon, in the photo-nuclear reactions such as

$$\gamma + {}^{124}\mathrm{Xe} \Longrightarrow {}^{123}\mathrm{I} + n\,,$$
$$\gamma + {}^{237}\mathrm{Np} \Longrightarrow {}^{236m}\mathrm{Np} + n\,,$$

and so on [6, 16]. Further investigations in this way are believed to be carried out before long.

Aforesaid obtaining ^{99m}Tc out of ^{99}Mo typifies manufacturing the practicable radio-isotope due to decay of some preceding isotope, procured at the first step, in the photo-nuclear reaction (2.2).

The values of Y , $\mathcal{Y}$, $\mathcal{M}$ acquired in Secs. 4, 5 are believed to be of practical interest, which is discussed next. Let us here recollect that accuracy of our findings is at all the points

6. Findings consideration

Once, for all we have by now acquired, there emerge alluring prospects of the radio-isotopes photo-production around electron linear accelerators.

Hereafter we correlate and contrast salient features of the routine reactor-based radio-isotope production, even though with the conversion from the HEU- to LEU-targets, and the electron accelerator-based radio-isotope production, addressing advantages of the last, specifically with respect to the case of recovery of ^{99}Mo and ^{99m}Tc, which are by far the major medical isotopes salable and consumed to-day [4, 7, 9, 10]. We follow the timely industry convention, and quantify the radio-isotope production and supply in terms of *6-day curies per week* [7, 9, 10], which is nominally the quantity of ^{99}Mo activity remaining 6 days after the recovered ^{99}Mo leaves the producer's facility, provided the ^{99}Mo has been elaborated during one week, and then was refined and processed before shipment to the market.

Let the electron beam with $J[\mathrm{A/cm^2}]$ and $\bar{E}_e = 50\,\mathrm{MeV}$ (see Fig. 1) irradiate the tungsten converter with $R_{\mathrm{W}} = 0.3\mathrm{cm}$, and the $\gamma-$flux, converted from this electron beam, produce the isotope Mo^{99} in the Mo sample, with $R_{\mathrm{Mo}} = 2\mathrm{cm}$ and $1\mathrm{cm}^2$ area, amenably to the photo-nuclear reaction (4.1). Then, with allowance for the time-dependence of Y (3.15), $\mathcal{Y}$ (3.16), $\mathcal{M}$ (3.17) (see Fig. 3), and the data given by tables 2, 3, we infer that the total yield of activity by the end of exposition would be

$$\mathcal{Y}(T_e, J_e, \mathcal{A}_{bn}) = J_e \cdot T_e \cdot \mathcal{A}_{nb} \cdot 1.7 \cdot 10^{11}\mathrm{kBq} \approx 5 \cdot 10^3 \cdot J_e \cdot T_e \cdot \mathcal{A}_{bn}\,\mathrm{Ci}, \tag{6.1}$$

provided the exposition time $T_e \lesssim 15\mathrm{h}$. At $T_e = 1\mathrm{h}$ and $J_e = 1\mathrm{A/cm^2}$, we have got the value (4.2) given above. The accelerator can be turned on and off at will and without any consequences, and exchanging the irradiated targets is rather a simple thing, which are apparent advantages of the accelerator-based radio-isotope production over the routine reactor-based one. So we are in position of irradiating a set of Mo targets successively, one after the other with the exposition time of each one equal to the most efficient value $T_e \approx 15\mathrm{h}$. Then, the yield of activity produced in every one of those samples is

$$\mathcal{Y}(15\mathrm{h}, J_e, \mathcal{A}_{bn}) \approx 5 \cdot 10^3 \cdot J_e \cdot 15 \cdot \mathcal{A}_{nb}\,\mathrm{Ci}, \tag{6.2}$$

As understood, this way leads to the greatest yield of activity generally attainable during a

total exposition time consumed in one week constitutes $\approx$ 150h. That series of ten targets expositions results in the total yield of activity per one week

$$\mathcal{Y}(10{\times}15\mathrm{h}, J_e, \mathcal{A}_{bn}) \approx 5 \cdot 10^3 \cdot J_e \cdot 15{\times}10 \cdot \mathcal{A}_{nb}\,\mathrm{Ci}, \tag{6.3}$$

As observed, this total activity is accumulated in the separated samples, taken together. On the other hand, we can continually irradiate one single sample one week long, *i.e.* again for $\approx$ 150h. In this case the evaluation accordingly Sections 3, 4 (Fig. 3, table 3) results in the total yield of activity accumulated per one week in that single target

$$\mathcal{Y}(150\mathrm{h}, J_e, \mathcal{A}_{bn}) \approx 3.2 \cdot 10^3 \cdot J_e \cdot 150 \cdot \mathcal{A}_{nb}\,\mathrm{Ci}, \tag{6.4}$$

which shows up to be noticeably smaller than the quantity (6.3). Let us opt a realizeable value $J_e = 10\mathrm{mA/cm}^2$, and presume that we operate targets composed of the pure isotope ^{100}Mo, *i.e.* $\mathcal{A}_{bn} = 1$ in the expressions (6.1)-(6.4). Then we arrive at

$$\mathcal{Y}(10{\times}15\mathrm{h}, 10\mathrm{mA}, 1) \approx 7.5 \cdot 10^3\mathrm{Ci}, \tag{6.5}$$

$$\mathcal{Y}(150\mathrm{h}, 10\mathrm{mA}, 1) \approx 4.8 \cdot 10^3\mathrm{Ci}. \tag{6.6}$$

Recalling $\tau_{^{99}\mathrm{Mo}} = 96\mathrm{h}$, the aforesaid *6-day curies* activities corresponding to the quantities (6.5), (6.6) are directly evaluated

$$\mathcal{Y}_{6-day}(10{\times}15\mathrm{h}, 10\mathrm{mA}, 1) \approx 1.67 \cdot 10^3\mathrm{Ci}, \tag{6.7}$$

$$\mathcal{Y}_{6-day}(150\mathrm{h}, 10\mathrm{mA}, 1) \approx 1.07 \cdot 10^3\mathrm{Ci}. \tag{6.8}$$

These quantities (6.5)-(6.8), evaluated with practicable ^{100}Mo targets and a realizable electron beam, prove to be competitive with the marketable *large-scale* productivity of the *large-scale producers*, who furnished on the market more than 1000 *6-day curies* of ^{99}Mo *per week*, recovered on the routine reactor basis with operating HEU targets [7].

Nowadays, the pure laboratory study [14–17] of the processes (4.1), (4.4), (4.6), with using foils of natural Mo , Sn , U as irradiated targets, have blazed the trail towards *the large-scale* radio-isotope manufacturing based on the electron-accelerator driving photo-neutron nuclear

In reactor-based radio-isotope producing, no matter whether the HEU- or LEU-target is used, the quantity of ^{99}Mo available for sale and harnessing is much less than the total quantity of ^{99}Mo produced in an irradiated target because of this 6 day delay and, primarily, because of losses caused by the very sophisticated and time-consuming target processing, still before shipment to the market. Upon irradiating and then cooling, the targets are processed into *hot cells facilities*, which can cost as much as tens of millions of dollars to construct, and which are very sophisticated to operate [7, 11]. The point is to recover a thoroughly purified desired radio-isotope (for instance ^{99}Mo) out of a target where this constitutes, at best, a few per cent among ^{235}U fission fragments [34]. In particular, the isotope ^{99}Mo, several hours after a moment of fission, constitutes $\sim 6\%$ of fission fragments. The other way round, in the accelerator-based photo-neutron production, there requires no *hot-sells* and subsidiary equipment for targets processing after the end of exposition, as a matter of fact. As well, the desired isotope, *e.g.* ^{99}Mo, is immediately elaborated within a pure molibdenium target, so that there is no need to purify anything and manage any wastes. Therefore the aforesaid 6-day term for calibrating activity of the shipment (*6-day curies*) is to be recounted just from the end of target exposition.

Used either HEU- or LEU-target, one of the most important issue to take care of is anyway to eliminate, or at least to minimize, the weapon-usable waste streams resulting from radio-isotope production. In particular concern is that little or no progress is being made for now in this way. Only a very small fraction, typically about 3%, of the ^{235}U in a target undergoes fission in reactor-based radio-isotope, *e.g.* ^{99}Mo, producing [7, 11]. The vast majority of the uranium in the target, along with other fission products and target materials, are eventually treated as wastes, no matter whether the HEU- or LEU-target is used. Tens of kilograms of HEU wastes are annually accumulated worldwide. By contrast, the electron-accelerator-based radio-isotope production has nothing to do with any radioactive wastes, there is no waste stream at all, in actual fact.

The decay product of ^{99}Mo, the isotope ^{99m}Tc (see Section 5), we are primarily focused on, is used in about two-thirds of all the diagnostic and therapeutic nuclear-medical procedures all over the world [5, 9, 11, 12]. The metastable radio-isotope ^{99m}Tc having got the short life-time, the ^{99}Mo recovered out of an irradiated target is shipped to radio-pharmacies and hospitals within the *technetium generators* that are *eluted* to obtain the desired ^{99m}Tc at

that are contained in a *generator* on the day of, or the day after its delivery to an user [4, 7, 11]. In the considered photo-neutron radio-isotope production, an irradiated Mo target could be processed in the *Tc-generator* just after the end of exposition, which is again an evident advantage over the routine reactor-based production, as the last requires a considerable time and work to prepare that irradiated HEU- or LEU-target for usage in the *Tc-generator*. Of course, the appropriate required *Tc-generator* is anew to be designed and built for recovering ^{99m}Tc from an irradiated Mo sample, upon photo-producing the ^{99}Mo radio-isotope therein, instead of the routine *Tc-generator* to process the blend of different Mo isotopes extracted out of ^{235}U fission fragments. The findings explicated in Section 5 will serve for all these actual purposes. The method how to recover the Tc from Mo irradiated targets are by now elaborated as well [8, 36].

As readily understood [7], refurbishing the obsolent reactors and converting from HEU-based to LEU-based radio-isotope production would be anyway time consuming, at least 5-6 years long, and technically sophisticated, at least not less than to bring online the accelerator-based radio-isotope production. Along with other complexities, the conversion would anew require the very expensive construction of the special *hot-cells* for processing now the LEU-targets, which are not involved at all into the accelerator-based photo-neutron radio-isotope production.

In the routine radio-isotope reactor-based elaboration, there is a very long implicated and vulnerable supply chain of manifold operations, beginning with the HEU provision of targets producers and terminating in treating end-users. Any contingency in a single link results in a fatal malfunction of all the chain, all the more that diverse operations are performed at different sites, in different countries, and even at different continents. In contrast, radio-isotope photo-neutron production would be accomplished at one single site: from an unsophisticated target preparation straightforwardly to radio-pharmaceutical manufactures, or, as *e.g.* in the ^{99}Mo production case, to charging the *Tc-generator*. There is no issue of shipment of the ^{99}Mo product to the ^{99m}Tc *generator* manufacturing facilities. The losses of radio-isotope yield caused by decay rate would be then minimized, and even almost eliminated, by co-locating all the engaged facilities. Under such circumstances, any irradiated ^{100}Mo target, upon utilizing by *Tc-generator*, would be restored, and then exposed anew. A circle of this kind could many times be repeated which would allow saving the stick of

agenda would offer the possibility of self-contained generator systems being feasible for central radio-pharmaceutical labs for a grope of hospitals. So, for all we have acquired, there offers a new stream from ^{99}Mo production to an end-user consumption of *kits* prepared with ^{99m}Tc.

As understood, see Section 4, the nuclear photo-neutron process $A(Z,N)(\gamma,n)A'(z,N-1)$ can serve to produce the great variety of desired radio-isotopes, not only with $A \sim 100$, $A \sim 140$, *i.e.* not only with A placed within the humps of mass distribution of uranium fission fragments. Especially, it is to indicate the isotope ^{201}Tl, that is thought to replace ^{99}Mo/^{99m}Tc usage, and a number of specific radio-isotopes used in the positron emission tomography (PET), ^{13}N, ^{18}F, ^{82}Sr/^{82}Rb, ^{45}Ti, ^{60}Cu, and so on [35], which are not available in the uranium fission process.

The above discussions are leading to consideration of building new and operating to-day existing electron linear accelerators (e-linacs) for the radio-isotope production. As understood, see Eqs. (6.1)-(6.8), the for now deployed $1/2MW$ e-linac $TRIUMF$ [11, 37], with electron energy $E_e = 50\,\mathrm{MeV}$ and current density $J_e = 10\mathrm{mA/cm}^2$ can be considered to be eligible for manufacturing 1000 *6-day curies* ^{99}Mo *activity per week*, *i.e.* for the *large scale* ^{99}Mo production. So, a single machine of this kind could manufacture and supply the ^{99}Mo marketable quantity comparable to productivity of a single *large scale* producer, provided the required ^{100}Mo pure targets are available. The manifold efficient methods and technologies to separate various isotopes are by now developed and deployed, see *e.g.* Refs. [6, 8]. So, recovery of a pure singe-isotope target, *e.g.* the pure ^{100}Mo isotope target, is believed to be not over-expensive, when the *large scale* radio-isotope photo-neutron manufacture would be validated.

Laboratories around the world, such as $TRIUMPF$ (Canada), BNL, $ORNL$ (U.S.), IRN-Orseay, $GANIL$ (France), $ELBE$ (Deutshland) [37–39], have expertise and facilities that can be used immediately. The construction of far more powerful e-linacs, with $E_e = 50\,\mathrm{MeV}$, $J_e = 100\mathrm{mA/cm}^2$, are by now under way, and they are believed to be commissioned before long, in 3-4 years, which would underpin a long-term enhancement of desired radio-isotopes production [11]. The estimated cost of such new accelerator is about \$50 millions, whereas the cost of an research and test reactor, with the thermal neutron flux $\approx (10^{14} - 10^{15})\mathrm{n/(s\ cm}^2)$, is assessed to be at least \$300-\$400 millions. For instance, construction cost

of euros [7]. Just fixing the $MAPLE$ reactors would have cost tens of millions of dollars, whereas building such new reactor or refurbishing NRU would have cost hundreds of millions of dollars. Even 5-years license extension for NRU would have required expenditure of about hundred of millions of dollars [7, 11]. Similarly, the reactor operations are far more costly than the e-linac operations. Power consumption, dominating the operating costs, is roughly estimated to be a few MWs for an aforesaid e-linac, and the total operating costs are assessed to constitute about 10% of the capital investment. Such an accelerator facility, as treated above, would be viewed as a single-purposed facility operating strictly for radio-isotope production business.

The γ-flux, converted from electron beam of an electron accelerator, can also be used for the photo-fission of ^{238}U , utilizing the natural or depleted uranium targets, with subsequent recovering the desired radio-isotope, *e.g.* ^{99}Mo , from the fission fragments blend [11]. The heretofore treated photo-neutron production of radio-isotopes is certain to be far more efficient and viable than the radio-isotope recovery out of the fission fragments of the ^{238}U photo-fission. In order to grasp the reason one is first to recollect that cross-sections $\sigma_{\gamma n}$ of the reaction (2.2) are akin the cross-section $\sigma_{\gamma f}$ of the ^{238}U photo-fission, both being of the same order [40]. Target nuclear densities are of the same order as well. Yet the desired radio-isotope, *e.g.* ^{99}Mo , constitutes at best only a few per cent, never more than $\sim (5-6)\%$, among ^{238}U photo-fission fragments. Thus, given the γ-flux causing both reactions is the same, the yield of photo-neutron reaction proves to be far more abundant than one from processing the irradiated ^{238}U sample upon the ^{238}U photo-fission. Anyway, the anew target processing and generator-manufacturing facilities are to be deployed, in using both photo-production, $^{100}\mathrm{Mo}(\gamma, n)^{99}\mathrm{Mo}$, and photo-fission ^{238}U process, $^{238}\mathrm{U}(\gamma, \mathrm{F})$. Yet although by this ^{99}Mo photo-fission production, just alike in the photo-neutron process, the accelerator does not produce radioactive waste from its operation, the waste from the irradiated targets chemical processing to recover, extract and purify ^{99}Mo would be similar to the waste of the reactor-based production. The ^{99}Mo recovery from ^{238}U photo-fission fragments and from ^{235}U thermal-neutron fission fragments are actually analogous. In either methods, the capital investments emerge to be very high, as the special facilities, in particular the *hot-sells*, are required to deal with the emission and disposal of highly radioactive fission products. In contrast, in the radio-isotope photo-neutron production, there are neither uranium fission

producing, there occur no secondary trance-uranic nuclei, in particular ^{239}Pu, associated with radio-isotope producing based on the ^{238}U photo-fission. As understood, see Eqs. (6.1)-(6.8), the mass of about 20g of 100% enriched ^{100}Mo is quite sufficient to design a practicable target for the large-scale ^{99}Mo photo-neutron production, whereas an depleted ^{238}U target for the photo-fission radio-isotope production would require the mass of at least $\sim$ 200g [11]. This large target mass is a substantial challenge in procuring required purity of the obtained medical radio-isotopes. Contamination possibility of a produced radio-isotope, *e.g.* ^{99}Mo , even increases due to the much larger mass of the photo-fission ^{238}U target as compared to the mass of the ^{235}U target in the case of the thermal neutron fission. So, as it has been coming to light, the photo-neutron production techniques has got a lot of advantages over the photo-fission one. Surely, it is least of all to say that these two approaches rule each other out. They are naturally to complement each other to procure the most reliable radio-isotope supply.

Further calculations and laboratory measurements are required to verify and validate the proof-of-principles that have been treated in the work presented.

Acknowledgments

Authors are thankful to O.D. Maslov, Z. Panteleev, Yu. P. Gangrsky for the valuable discussions.

---

[1] Isotope Production and Application in the 21st Century. Proceedings of the Third Internal Conference on Isotopes, Vancouver, Canada, 6-10 September, 1999. Would Scientific Pub. Co. In. Vancouver, B.C. Stevenson, 2000.

[2] F.F.R. Knapp, S. Mirzadeck, et all., Journal of Radioanalytical and Nuclear Chemistry 263 (2005) 503.

[3] Isotope Production and Applications. Workshop on the Nation's Needs for Isotopes: Present and Future. Rockwille, MD, August 5-7 2008. U.S. Depatament of Energy, 2008.

[4] Isotopes for Medicine and Life Science. Committee on Biomedical Isotopes. Ed. S.J.Adelstein, F.J. Manning. National Academies Press, Washington D.C., 1999.

[6] M.J. Rivard, L.M. Bodeck. R.A.Butler, et all., Applied Radiation and Isotopes 63 (2005) 157.

[7] Medical Isotope Production without Highly Enriched Uranium. National Research Council of the National Academies. C.G. Whippl (chair). The National Academies Press, Washington, D.C. 2009.

[8] I.N. Bekman, Radioactivity and Radiation (Lecture 7). Moscow State University, Moscow, 2006;

T. S. Bigelow, et al., Production of stable isotopes utilizing the plasma separation process, WILEY, Inter Science, 2005;

M. D. Matthews, Systems and Methods for Isotope Separation. Pub. No.: U.S. 2007/0272557 A1, Nov. 29, 2007.

[9] R.W. Atcher, Journal of Nuclear Medicine, 50 (2009) 17N.

[10] C.R. Goldfarb, S.R. Rarmett, L. Zuckier, Nuclear Medicine Board Review, Thieme, National Academies Press, Washington, D.C. 2007.

[11] Making Medical Isotopes. Report of the Task Force on Alternatives for Medical-Isotope Production. Ed. A. Fong, T.I. Meyer, K. Zala. AAPS, Canada, TRIUMF, 2008.

[12] D. Akin, Edmonton Journal, May 21 (2009).

[13] S. West, CBC News, January 16, 2008.

[14] A.B. Sabel'nikov, O.D. Maslov, et al., Radiochemistry 48 (2006) 191.

[15] A.B. Sabel'nikov, O.D. Maslov, et al., Radiochemistry 48 (2006) 187.

[16] S.N. Dmitriev, O.D. Maslov, A.B. Sabel'nikov, et al., Radiochemistry 40 (1998) 552.

[17] S. N. Dmitriev, N.G. Zaitzeva, Radiochemica Acta, 93 (2005) 571.

[18] Landolt-Börnstein, Elementary Particles, Nuclei and Atoms, 16 A, Ed. by H. Shopper, Springer, 2000;

A. B. Migdal, The Theory of Finite Fermi Systems and the Nuclei Properties, "Nauka", Moscow, 1965.

[19] A. I. Akhiezer, V.B. Berestetskii, Quantum Electrodynamics, "FM", Moscow, 1959.

[20] W. Heitler, The Quantum Theory of Radiation, Clarendon press, Oxford, London, 1954.

[21] V.B. Berestetskii, E.M. Lifshits L. P., Pitaevskii, Relativistic Quantum Theory, Pergamon, Oxford, 1971.

[22] L.I. Shiff, Phis.Rev. 83 (1951) 252.

[23] H. Bethe and W. Heitler, Proc. Roy. Soc. A 146 (1934) 83.

[24] The Nuclear Handbook, Ed. O.R. Frisch, George Newnes Limited, London, 1958;
The Table s of Physical Quantities, Ed. I.K. Kikoin, "Atomizdat", Moscow, 1976.
[25] J.F. Carlson, J.R. Oppenheimer, Phys.Rev. 51 (1936) 220;
H.J. Bhabha, W. Heitler, Proc. Roy. Soc., A 159 (1936) 432;
L. Jànossy Cosmic Rays. Oxford, 1948.
[26] M. Ericson, M. Rosa-Clot, Z. Phys. A 324 (1991) 373;
B. Baumann, et al., Phys. Rev. C 38 (1988) 1940;
E.Hayward, Phys. Rev. C 40 (1989) 467.
[27] S. C. Srivastava, et al., Nuclear Medicine and Biology Advances, Ed. C. Raynaud, Pergamon Press, London, 1983.
[28] H. Beil, et al., Nucl. Phys. A 227 (1974) 427.
[29] S. C. Srivastava, et al., Clinical Cancer Research 4 (1998) 61.
[30] A. Lepretre, et al., Nucl. Phys. A 219 (1974) 39.
[31] Ch. Berthelot, et al., Proc. Modern Trends in Activation Analysis, Copenhagen V. 1, (1986) 663.
[32] A. Veyssiere, H. Beil, R. Berger, et al., Nucl.Phys. A 199 (1973) 45;
J.T. Caldwel, E.J. Dowdy, B.L. Berman, Phys. Rev. C 21 (1980) 1215.
[33] C. M. Lederer, et al., Table of Isotopes, J. Wiley and sons, INC, New York, London, Sydney, 1968;
F.D.Sowby, Radionuclide Transformations: Energy and Intensity of Emission. ICRP Publication 38, Pergamon, 1983;
Nuclear Data Services.//www-nds.iaea.org/ENSDF
[34] S. Katcoff, Nucleonics, 18 (1960) 201;
Yu. A. Ziskin, A. A. Lbov, L. I. Sel'genkov Fission Products and their mass distributions. GOSATOMIZDAT, Moscow, 1963;
Yu. P. Gangrsky, B. N. Markov, V. P. Pereligin, Fission Fragments Registration and Spectrometry. Energoatomizdat, Moscow, 1992.
[35] J.Lewis, et all., Q. J. Nucl. Med. Mol. Imaging, 52(2) (2008) 101;
S. Jurisson, et all., O. J. Nucl. Med. Mol. Imaginig, 52 (2008) 222.
[36] V. S. Skuridin, E. V. Chibisov, Patent RF $\mathcal{N}$ 2161132, 27.12.2000. // ru-patent. info/21/60-64/2161132htm .

[37] S. Koscielniak, F. Ames, Y. Bylinsky, et al., in: Proceedings of EPAC08, 11h European Particle Accelerator Conference, Genoa, Italy, June 23-27, 2008., TRI-PP-08-06, August 2008.

[38] K.H. Guber, T.S. Bigelow, C. Ausmus, et al., Int. Conf. on Nucl. Data for Science and Technology 2007, EDP Sciences, 2008. (http://nd2007.edpsciences.org).

[39] E. Altstadt, C. Beckert, H. Freiesleben, et al., Annals of Nuclear Energy 34 (2007) 36;
C. Kaya, U. Lehnart, Proceedings of DIPAC09, Basel, Sw. June 2009.

[40] A.Veyssiere, et al., Nucl. Phys. A 199 (1973) 45;
J.D.T. Arrudantro, et al., Phys. Rev. C 14 (1976) 1499;
J.T. Caldwell, et al., Phys. Rev. C 21 (1984) 1215.

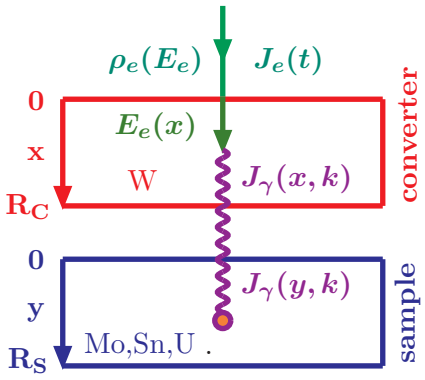

Fig. 1. The setup scheme.

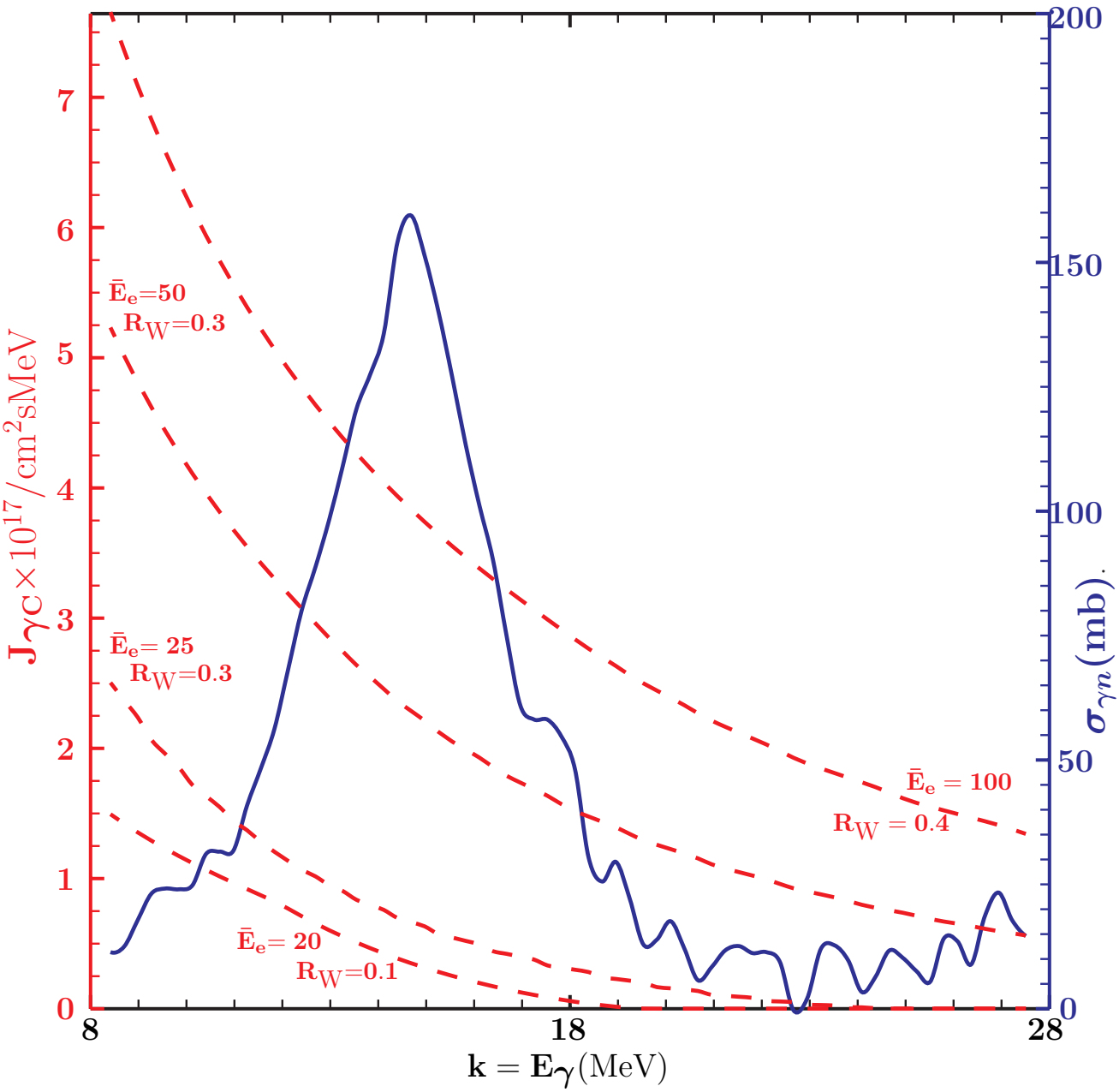

Fig. 2. The dashed curves represent the k-dependence of the γ-flux (2.22) at the final edge of converter for various $\bar{E}_e$(MeV) and the most preferable thicknesses R_W(cm), which are plotted alongside the respective curves. The electron energies are distributed around the given $\bar{E}_e$(MeV) accordingly Eq. (2.23) with the E_e^b, E_e^u, Δ_e values chosen as in table 5. The initial electron current density $J_e = 1\text{A/cm}^2$. The solid curve represents k-dependence of the cross-section of reaction in Eq. (4.1).

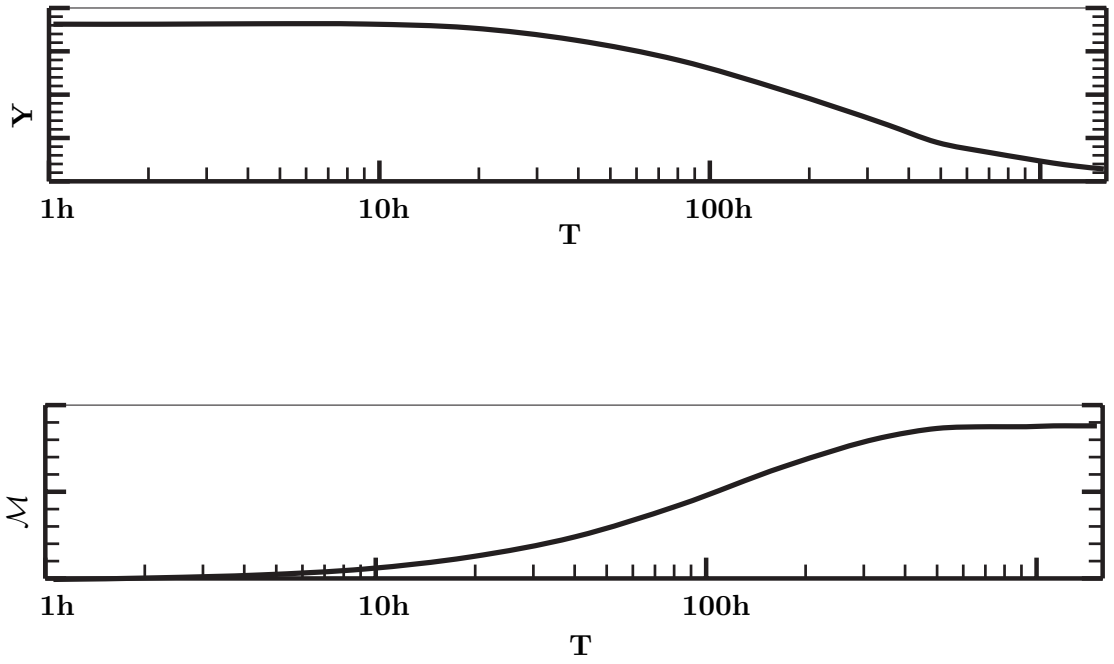

Fig. 3. Time dependence of the yield of activity $Y[\mathrm{Bq}/(\mathrm{h}\cdot\mu\mathrm{A}\cdot\mathrm{mg}\,^{100}\mathrm{Mo})]$ and amount $\mathcal{M}(\mathrm{mg}10^{-1})$ obtained with the converter thickness $R_W = 0.3\mathrm{cm}$ by irradiation of the natural $^{nat}\mathrm{Mo}$ sample, with $1\mathrm{cm}^2$ area and thickness $R_{\mathrm{Mo}} = 0.01\mathrm{cm}$ (foil), by electrons with $\bar{E}_e = 25\,\mathrm{MeV}\,,\ J_e = 1\mathrm{A}/\mathrm{cm}^2$.

Table 1

The yield of activity $Y[\mathrm{kBq}/(\mathrm{h}\cdot\mu\mathrm{A}\cdot\mathrm{mg}\,^{100}\mathrm{Mo})]$ and amount $\mathcal{M}(\mathrm{mg}10^{-2})$ of ^{99}Mo at various converter thickness $R_W(\mathrm{cm})$, upon irradiating the natural ^{nat}Mo sample, with $1\,\mathrm{cm}^2$ area and $R_{\mathrm{Mo}} = 0.01\,\mathrm{cm}$ (foil), by electrons with $E_e = 25\,\mathrm{MeV}$, $J_e = 1\mathrm{A}/\mathrm{cm}^2$, during 1h.

R_{W}	0.1	0.15	0.175	0.2	0.25	0.30
Y	3.63	4.09	4.07	3.99	3.80	3.62
$\mathcal{M}$	0.18	0.2	0.2	0.196	0.187	0.177

Table 2

The yield of activity $Y[\mathrm{kBq}/(\mathrm{h}\cdot\mu\mathrm{A}\cdot\mathrm{mg}\,^{100}\mathrm{Mo})]$ and amount $\mathcal{M}(\mathrm{mg}10^{-2})$ of the ^{99}Mo at various sample thickness $R_{\mathrm{Mo}}(\mathrm{cm})$, upon irradiating the natural ^{nat}Mo sample during 1h by electrons with $E_e = 25\,\mathrm{MeV}$, $J_e = 1\mathrm{A}/\mathrm{cm}^2$, with the converter thickness $R_W = 0.15\,\mathrm{cm}$.

R_{Mo}	0.01	0.5	1.0	1.5	2.0	4.0
Y	4.09	3.75	3.44	3.17	2.93	2.186
$\mathcal{M}$	0.2	9.2	16.8	23.4	28.65	42.9

continuing

R_{Mo}	6.0	8.0	10.0	12.0	14.0
Y	1.69	1.37	1.12	0.948	0.818
$\mathcal{M}$	49.73	53.3	55.0	56.2	56.8

Table 3

The same as in table 2, yet for $R_W = 0.3\,\mathrm{cm}$, and for the initial electron energy distributed around $\bar{E}_e = 50\,\mathrm{MeV}$ accordingly Eq. (2.23) with $E_e^b = 48.5\,\mathrm{MeV}$, $E_e^u = 52.5\,\mathrm{MeV}$, $\Delta_e = 0.5\,\mathrm{MeV}$.

R_{Mo}	0.01	0.5	1.0	1.5	2.0	2.5
Y	11.73	10.73	9.86	9.07	8.37	7.78
$\mathcal{M}$	0.58	26.3	48.4	66.8	82.2	94.4

Table 4

The same as in table 3, yet for $R_W = 0.4\,\mathrm{cm}$, and for the initial electron energy distributed around $\bar{E}_e = 100\,\mathrm{MeV}$ accordingly Eq. (2.23) with $E_e^b = 95\,\mathrm{MeV}$, $E_e^u = 105\,\mathrm{MeV}$, $\Delta_e = 1\,\mathrm{MeV}$.

R_{Mo}	0.01	0.5	1.0	1.5	2.0	2.5
Y	19.45	17.80	16.33	15.03	13.84	12.82
$\mathcal{M}$	0.95	43.7	80.1	110.6	136.1	157.2

Table 5

The yield of activity $Y[\mathrm{kBq}/(\mathrm{h}\cdot\mu\mathrm{A}\cdot\mathrm{mg}\,^{100}\mathrm{Mo})]$ and amount $\mathcal{M}(\mathrm{mg}10^{-2})$ of ^{99}Mo at various initial electron energy distributions described by $\bar{E}_e$, E_e^b, E_e^u, Δ_e, all in MeV, as given in Eq. (2.23), and at the most preferable respective thicknesses $R_W(\mathrm{cm})$. The natural ^{nat}Mo sample, with the thickness $R_{\mathrm{Mo}} = 0.01\mathrm{cm}$ and $1\mathrm{cm}^2$ area, is irradiated by the electron current $J_e = 1\mathrm{A}/\mathrm{cm}^2$, during 1h.

$\bar{E}_e$	20	25	50	100
E_e^b	19.5	24.5	48.5	95
E_e^u	20.5	25.5	52.5	105
Δ_e	0.2	0.2	0.5	1.0
R_{W}	0.1	0.180	0.3	0.4
Y	2.0	4.09	11.73	19.45
$\mathcal{M}$	0.1	0.2	0.58	0.95

Table 6

The same as in table 5, yet here the quantities $Y[\mathrm{kBq}/(\mathrm{h}\cdot\mu\mathrm{A}\cdot\mathrm{mg}\,^{118}\mathrm{Sn})]$ and $\mathcal{M}(\mathrm{mg}10^{-2})$ are obtained for $^{117}\mathrm{Sn}^{m}$ production from the natural tin $^{nat}\mathrm{Sn}$ sample, with the thicknesses $R_{\mathrm{Sn}} = 0.01\mathrm{cm}$ (foil), $R_{\mathrm{Sn}} = 2\mathrm{cm}$, and $1\mathrm{cm}^2$ area.

$\bar{E}_e$	20	25	50	100
E_e^b	19.5	24.5	48.5	95
E_e^u	20.5	25.5	52.5	105
Δ_e	0.2	0.2	0.5	1.0
R_{W}	0.1	0.15	0.3	0.4
$Y,\ R_{\mathrm{Sn}} = 0.01$	0.456	1.04	3.18	5.48
$Y,\ R_{\mathrm{Sn}} = 2.0$	0.34	0.78	2.37	4.08
$\mathcal{M},\ R_{\mathrm{Sn}} = 0.01$	0.27	0.62	1.89	3.26
$\mathcal{M},\ R_{\mathrm{Sn}} = 2.0$	40.84	93.00	283.6	487.5

Table 7

The same as in table 6, yet the quantities $Y[\mathrm{kBq}/(\mathrm{h}\cdot\mu\mathrm{A}\cdot\mathrm{mg}\,^{238}\mathrm{U})]$ and $\mathcal{M}(\mathrm{mg}10^{-2})$ are obtained for ^{237}U produced from the natural ^{nat}U.

$\bar{E}_e$	20	25	50	100
E_e^b	19.5	24.5	48.5	95
E_e^u	20.5	25.5	52.5	105
Δ_e	0.1	0.1	0.5	1.0
R_{W}	0.15	0.20	0.35	0.45
$Y,\ R_{\mathrm{U}}=0.01$	1.01	1.77	4.08	6.64
$Y,\ R_{\mathrm{U}}=2.0$	0.45	0.78	1.78	2.89
$\mathcal{M},\ R_{\mathrm{U}}=0.01$	6.3	11.07	25.44	41.41
$\mathcal{M},\ R_{\mathrm{U}}=2.0$	558.4	978.9	2234	3626

Table 8

The time T_{max}(h) of maximum accumulation of the isotope ^{99m}Tc and the respective yield of activity $Y[\mathrm{kBq}/(\mathrm{h}\cdot\mu\mathrm{A}\cdot\mathrm{mg}\,^{100}\mathrm{Mo})]$ and amount $\mathcal{M}_{\mathrm{Tc}^m}(\mathrm{mg}10^{-5})$, as functions on the time T_e(h) of irradiation of the natural ^{nat}Mo sample, with 1cm^2 area and $R_{\mathrm{Mo}}=0.01$cm (foil), by electrons with $J_e=1\mathrm{A/cm}^2$, $\bar{E}_e=25$MeV, at the converter thickness $R_W=0.3$cm.

T_e	0.5	1	5	10	15	20
T_{max}	20	23	25	28	30	32
Y_{Tc^m}	2.54	2.52	2.44	2.32	2.21	2.15
$\mathcal{M}_{\mathrm{Tc}^m}$	5.65	11.3	54.3	103	147	188

Table 9

The $T(h)$-dependence of the yield of activity $Y_{\mathrm{Tc}^m}[\mathrm{kBq}/(\mathrm{h}\cdot\mu\mathrm{A}\cdot\mathrm{mg}\,^{100}\mathrm{Mo})]$ and amount $\mathcal{M}_{\mathrm{Tc}_m}(\mathrm{mg}10^{-5})$ of $^{99m}\mathrm{Tc}$ which results inside the natural $^{nat}\mathrm{Mo}$ sample, with $1\mathrm{cm}^2$ area and the thickness $R_{\mathrm{Mo}} = 0.01\mathrm{cm}$ (foil), irradiated during $T_e = 0.5\mathrm{h}$ by electrons with $\bar{E}_e = 25\mathrm{MeV}\,,\ J_e = 1\mathrm{A}/\mathrm{cm}^2$; the converter thickness $R_W = 0.3\mathrm{cm}$.

T	0.5	1.5	5.0	10	20	30
Y_{Tc^m}	0.092	0.434	1.43	2.07	2.54	2.50
$\mathcal{M}_{\mathrm{Tc}^m}$	0.2	0.96	3.19	4.60	5.65	5.56

continuing

T	40	50	60	80	100
Y_{Tc^m}	2.32	2.11	1.9	1.55	1.26
$\mathcal{M}_{\mathrm{Tc}^m}$	5.16	4.70	4.24	3.44	2.79

Table 10

The dependence of the yield of ^{99m}Tc activity Y_{Tc^m}[kBq/(h $\cdot$ μA $\cdot$ mg ^{100}Mo)] and amount $\mathcal{M}_{\mathrm{Tc}^m}(\mathrm{mg}10^{-5})$ on the thickness R_{Mo}[cm] of the natural ^{nat}Mo sample, with 1cm^2 area, irradiated during $T_e = 0.5$h by electrons with $J_e = 1\mathrm{A/cm}^2$, $\bar{E}_e = 25$Mev. The converter thickness $R_W = 0.3$cm. All the results are obtained at the time $T = 20$h, counting from exposition start.

R_{Mo}	0.01	0.5	1	2	4	6
Y_{Tc^m}	2.54	2.30	2.13	1.80	1.36	1.05
$\mathcal{M}_{\mathrm{Tc}^m}$	5.65	264	478	810	1209	1405

continuing

R_{Mo}	8	10	12	16	20
Y_{Tc^m}	0.84	0.7	0.59	0.45	0.36
$\mathcal{M}_{\mathrm{Tc}^m}$	1502	1549	1573	1590	1595

Table 11

The yield of activity $Y_{\mathrm{Tc}^m}[\mathrm{kBq}/(\mathrm{h}\cdot\mu\mathrm{A}\cdot\mathrm{mg}\,^{100}\mathrm{Mo})]$ and amount $\mathcal{M}_{\mathrm{Tc}^m}(\mathrm{mg}10^{-5})$ of ^{99m}Tc, evaluated at $T = T_e(\mathrm{h})$ and $T = T_{max}(\mathrm{h})$, the most preferable time of ^{99m}Tc extraction, for various initial electron energies $\bar{E}_e(\mathrm{MeV})$. The natural ^{nat}Mo sample, with $1\mathrm{cm}^2$ area and thickness $R_{\mathrm{Mo}} = 0.01\mathrm{cm}$ (foil), is irradiated during $T_e = 1\mathrm{h}$ by the current $J_e = 1\mathrm{A}/\mathrm{cm}^2$. R_W is the converter thickness, preferable at the given $\bar{E}_e$.

$\bar{E}_e$	20	25	50	100
R_{W}	0.1	0.15	0.3	0.4
T_{max}	23	23	23.5	24
$Y_{\mathrm{Tc}^m}(T_e)$	0.1	0.2	0.59	0.99
$Y_{\mathrm{Tc}^m}(T_{max})$	1.42	2.88	8.28	13.92
$\mathcal{M}_{\mathrm{Tc}^m}(T_e)$	0.45	0.91	2.62	4.4
$\mathcal{M}_{\mathrm{Tc}^m}(T_{max})$	6.29	12.79	36.8	61.82

Table 12

The same as in table 11, yet with $R_{\mathrm{Mo}} = 2\mathrm{cm}$.

$\bar{E}_e$	20	25	50	100
R_{W}	0.1	0.15	0.3	0.4
T_{max}	23	23	23.5	24
$Y_{\mathrm{Tc}^m}(T_e)$	0.07	0.15	0.42	0.71
$Y_{\mathrm{Tc}^m}(T_{max})$	1.02	2.06	5.90	9.91
$\mathcal{M}_{\mathrm{Tc}^m}(T_e)$	66.4	134	383	643
$\mathcal{M}_{\mathrm{Tc}^m}(T_{max})$	922	1858	5328	8941